

Fe₃O₄ Nanoparticles Prepared by Seeded-Growth Route for Hyperthermia: Electron Magnetic Resonance as a Key Tool to Evaluate Size Distribution in Magnetic Nanoparticles.

Idoia Castellanos-Rubio^a, Maite Insausti^{ab}, Eneko Garaio^c, Izaskun Gil de Muro^a, Fernando Plazaola^c, Teófilo Rojo^a, Luis Lezama^{*ab}

^aDpto. de Química Inorgánica, Universidad del País Vasco, UPV/EHU, P.O. Box. 644, E-48080, Bilbao, Spain.

^bBCMaterials, Parque Científico y Tecnológico de Bizkaia, E-48160, Derio, Spain.

^cDpto. Electricidad y Electrónica, Universidad del País Vasco, UPV/EHU, P.O. Box. 644, E-48080, Bilbao, Spain.

ASSOCIATED CONTENT

Table of contents

Table S1. Summary of solvent volume and reagent amounts used in each addition step for the synthesis of samples A-F, and their sizes after different growth steps.

Figure S1. **a)** Diffractograms of samples A-F. **b)** Deconvolution of (311) diffraction peak of Fe₃O₄ for samples A-F.

Table S2. Parameters obtained from deconvolution of (311) diffraction peak and calculated crystallite size using Scherrer equation.

Figure S2. FTIR spectra of (a) pure oleic acid and (b) Fe₃O₄ nanoparticles coated with oleic acid in sample D.

Figure S3. ZFC/FC curves of powder samples A-E, obtained under an applied field of 10 Oe.

Figure S4. Hysteresis loops at room temperature of powder samples A-F **a)**, **b)** and of colloidal dispersion embedded in polystyrene **c)**.

Figure S5. Hysteresis loops at 5 K of powder samples A-F **a)** and of colloidal dispersion embedded in polystyrene **b)**.

Model S1. Non-Interacting Super-Paramagnetic (SPM) model.

Figure S6. Fit of M(H) curves at room temperature by SPM model **a)** of powder samples (C and E) and **b)** of colloidal dispersion embedded in polystyrene (A-E).

Model S2. Calculation of SAR as a function of mean diameter.

Figure S7. SAR values as a function of frequency under an AC magnetic field of 10 kA/m for sample E before and after washing process.

Table S1. Summary of solvent volume and reagent amounts used in each addition step for the synthesis of samples A-F, and their sizes after different growth steps.

Sample <i>D</i> / nm	Growth step	Dibenzyl ether /ml	Seed	1,2- hexadecanediol /mmol	Fe(CO) ₅ /mmol	RCOOH /mmol	R-NH ₂ /mmol
A 4.3	1	20	--	20	0.75	1	6
B 7.7	3	20	--	20	1. 0.75 2. 3.3 3. 7.7	1. 1 2. 2 3. 3.25	1. 6 2. 6 3. 6
D 11.9	4	20	--	20	1. 0.75 2. 3.3 3. 7.7 4. 14	1. 1 2. 2 3. 3.25 1. 4.3	1. 6 2. 6 3. 6 1. 6
E 14.9	5	20	--	20	1. 0.75 2. 3.3 3. 7.7 4. 14 5. 22	1. 1 2. 2 3. 3.25 4. 4.3 5. 5.44	1. 6 2. 6 3. 6 4. 6 5. 6
F 11.1	5	20	--	10	1. 0.375 2. 1.65 3. 3.85 4. 7 5. 11	1. 0.5 2. 1 3. 1.625 4. 2.15 5. 2.72	1. 3 2. 3 3. 3 4. 3 6. 3
C 10.6	3+1	20	260 mg of sample B	15	4. 5.3	4. 7	4. 6

Figure S1_a. Diffractograms of samples A-E

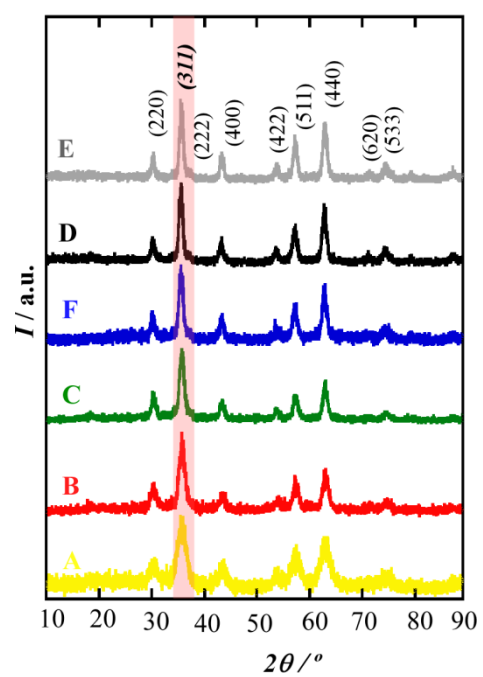
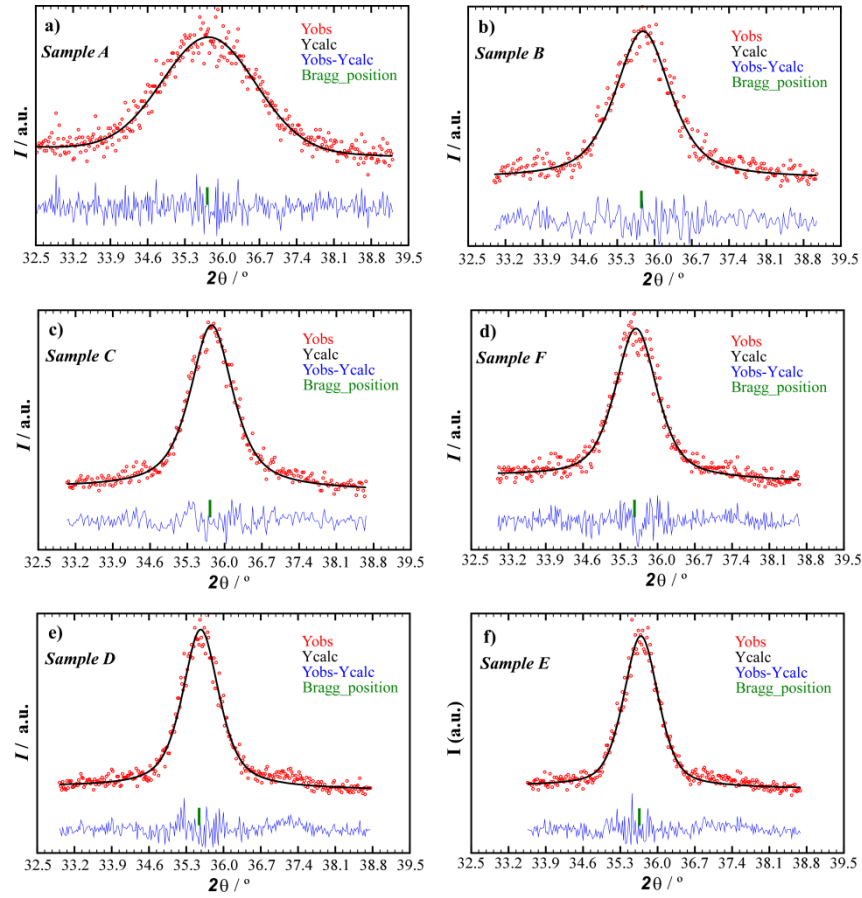


Figure S1_b. Deconvolution of (311) diffraction peak of Fe_3O_4 for samples A-F.



The crystallite size has been calculated by the deconvolution of the (311) diffraction peak and using the Scherrer equation (1):

$$D = \frac{K\lambda}{B_{\text{estruc.}} \cos \theta} = \quad (1)$$

Where K is the shape factor (0.95), $B_{\text{structure}} = B_{\text{observed}} - B_{\text{instrumental}}$, the full width at half maximum, $\lambda = (K\alpha_1 + K\alpha_2)/2 = 1.5418 \text{ \AA}$, and θ peak position.

Table S2. Parameters obtained from (311) diffraction peak deconvolution and calculated crystallite size using Scherrer equation*.

Sample	$B_{\text{obs.}}$ / °2θ	$B_{\text{inst.}}$ / °2θ	Peak pos. / °2θ	$B_{\text{struct.}}$ / °2θ	Crystallite size / nm
<i>A</i>	2.069	0.120	35.722	1.949	4.5(±0.5)
<i>B</i>	1.219	0.120	35.750	1.099	8.0(±0.5)
<i>C</i>	0.949	0.120	35.725	0.829	10.5(±0.5)
<i>F</i>	0.927	0.120	35.566	0.807	11.0(±0.5)
<i>D</i>	0.826	0.120	35.539	0.690	12.0(±0.5)
<i>E</i>	0.763	0.120	35.657	0.643	14.0(±0.5)

*Mean sizes have one significant digit due to the uncertainty of calculation.

Figure S2. FTIR spectra of (a) pure oleic acid and (b) Fe_3O_4 nanoparticles coated with oleic acid in sample D

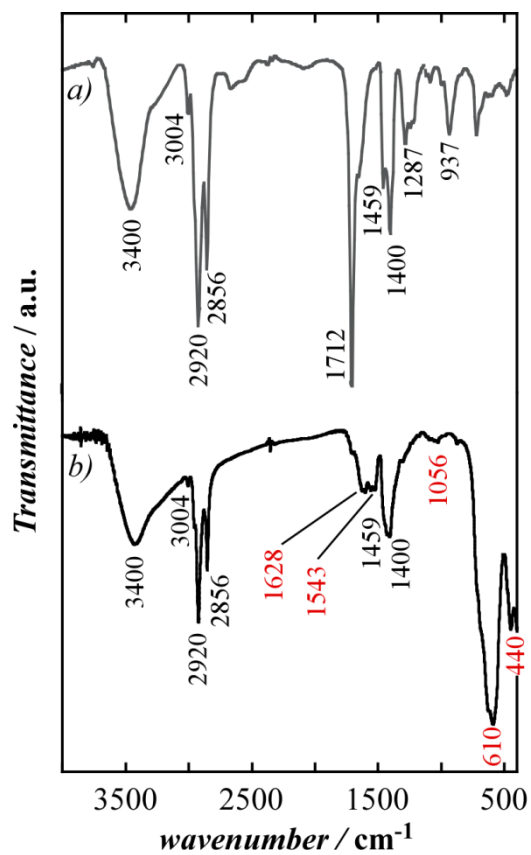


Figure S3. ZFC/FC curves of powder samples A-E, obtained under an applied field of 10 Oe.

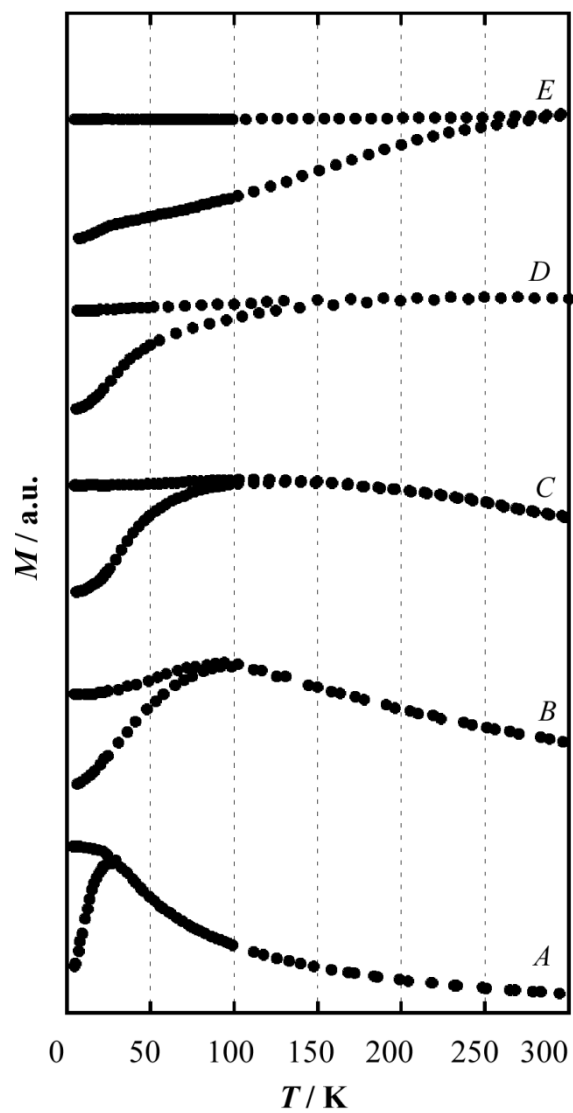


Figure S4. Hysteresis loops at room temperature of powder samples A-F **a)**, **b)** and of colloidal dispersion embedded in polystyrene **c)**.

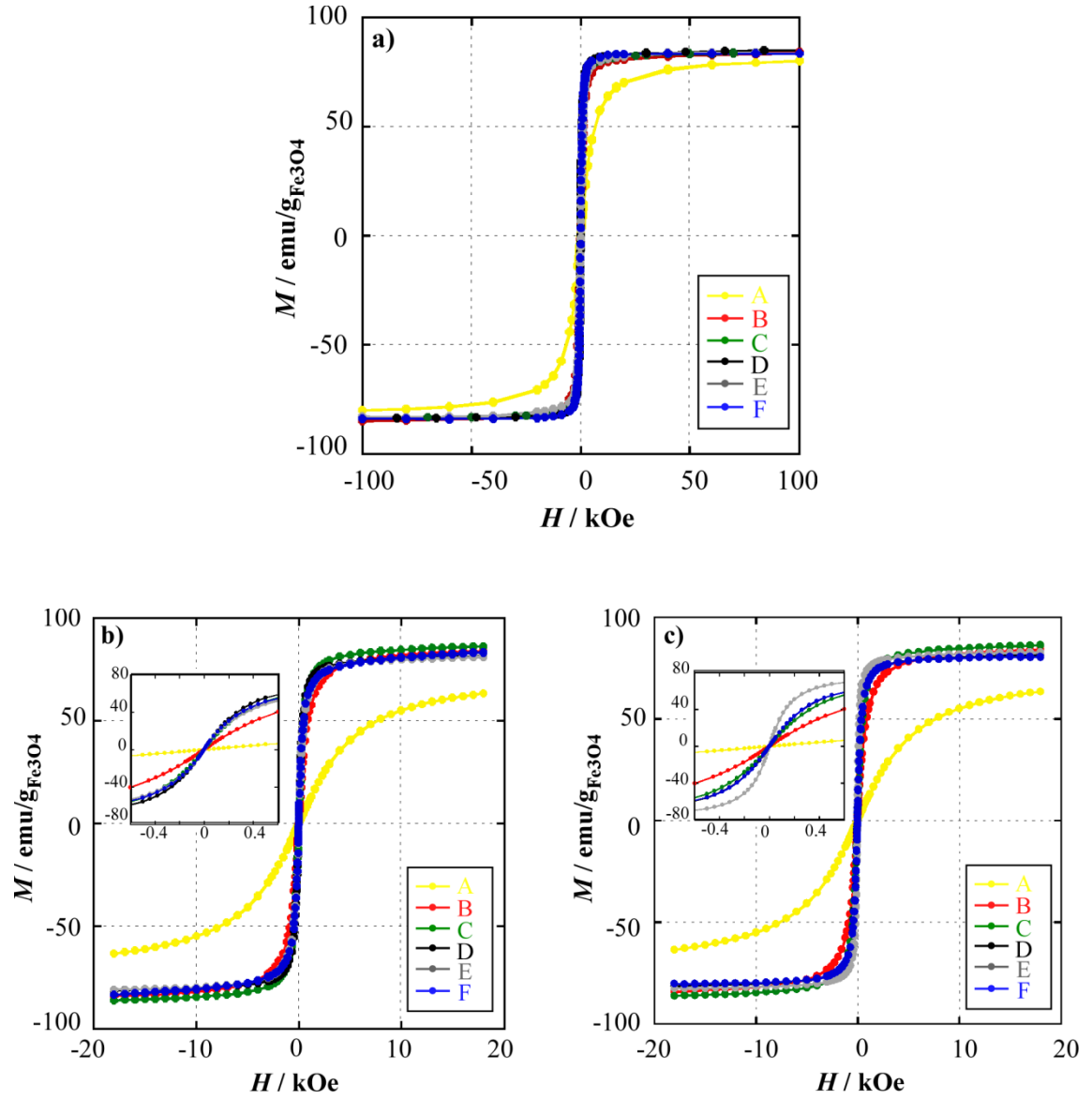
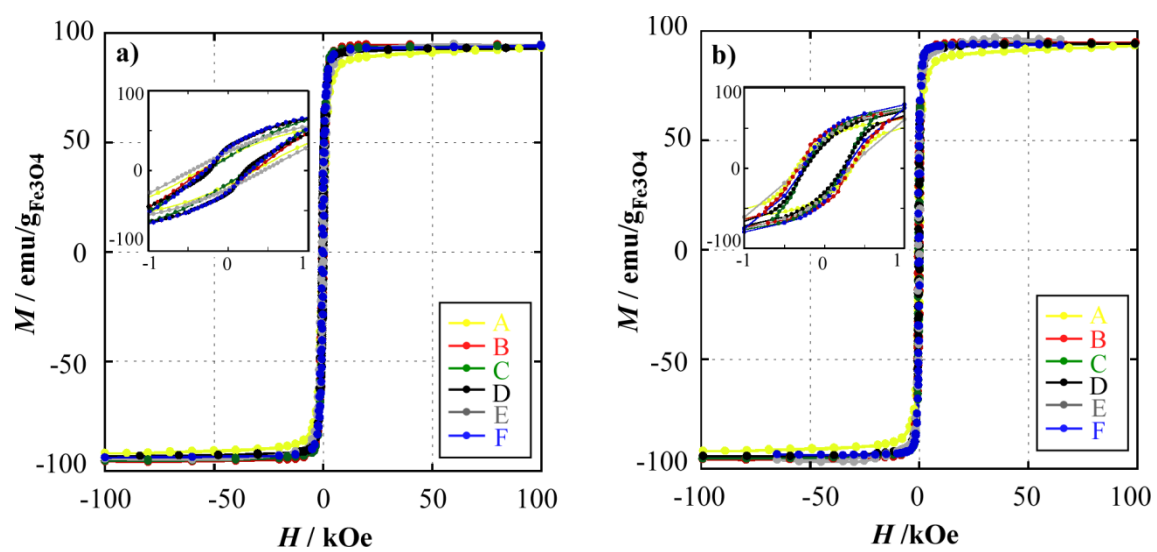


Figure S5. Hysteresis loops at 5 K of powder samples A-F **a)** and of colloidal dispersion embedded in polystyrene **b)**.



Model S1. Non-Interacting Super-Paramagnetic (SPM) model.

Magnetization in Single Domain Particles:

The present calculation of magnetization for an assembly of single magnetic domain particles is based in the following assumptions:

1. The population of nanoparticles is composed of single domains with uniaxial anisotropy, being their easy axes oriented at random.
2. Interparticle dipolar interactions are negligible so that the assembly is a set of independent single magnetic domains.

The second condition is quite hard to fulfill in a real nanoparticle system; as a consequence, in order to characterize the magnetic properties of individual particles, e.g. magnetic moment, size and effective anisotropy, the use of enough diluted samples becomes imperative, either by using small concentrated colloids or solid samples dispersed in non-metallic matrix.

Non-Interacting SPM model: magnetization as a function of external magnetic field.

Langevin equation.

Let us suppose a set of magnetic nanoparticles composed of single magnetic domains with their easy axis oriented in any direction of the space with equal probability, i.e., at random. Under the condition $k_B T \gg KV$, for a given T , the particles are in the superparamagnetic state (SPM) and for any particle, its energy (E_B) under an external magnetic field (H) is given by the scalar product of its magnetic moment μ by the magnetic field H : $E_B = -\mu H \cos\theta$. Classical Boltzman statistics states that the number of magnetic moments dn forming an angle between θ and $\theta + d\theta$ relative to the external magnetic field, is proportional to: $dA \exp(\mu H \cos\theta / k_B T)$, where the differential area is $dA = 2\pi \sin\theta d\theta$ (for a sphere of unit radius). In this way, it can be said that: $dn = C 2\pi \sin\theta d\theta \exp(\mu H \cos\theta / k_B T)$, where C is a proportionality constant fixed by the

normalizing condition: $\int_0^\pi dn = n$, the total number of particles.

The contribution of these magnetic moments to the whole is given by $\mu \cos\theta dn$, and therefore the total magnetization, will be the sum of these contributions:

$$M = 2\pi C \mu \int_0^\pi \sin\theta \cos\theta \exp(x \mu) d\theta$$
, where $x = \mu H / k_B T$. The integral can be solved analytically, and then the magnetization is finally given by: $M = n\mu(\coth(x) - 1/x)$. Considering that saturation magnetization $M_S = n\mu$, the function $M(H)$ will follow the so-called Langevin equation:

$$M(H) = M_S \left[\coth\left(\frac{\mu H}{k_B T}\right) - \frac{k_B T}{\mu H} \right] = M_S L\left(\frac{\mu H}{k_B T}\right) \quad (2)$$

Effect of size distribution.

In a real sample, the size of nanoparticles is not perfectly defined but is typically distributed around some value, a most probable size for instance. The analysis of TEM images usually supplies a histogram of sizes, i.e., a set of numbers, each of which represents a probability of finding that size in the assembly. Such size distributions can be usually fitted to Gaussian or Log-normal functions. In general, this probability function will be given by $f(D)$, so that the total magnetization of the assembly can be calculated as a sum (integral) over all the sizes (diameter D) in the distribution:

$$M(H) = M_s \int_0^{\infty} L\left(\frac{\mu H}{k_B T}\right) f(D) dD \quad (3)$$

where saturation magnetization, M_s , is the same for all the particles in the population. In principle, the saturation magnetization units are arbitrary because the only requirement is that M_s should match the experimental magnetization that can be normalized in different ways. Taking into account that $\mu = MV$, the final expression for the function $M(H)$ is the following one:

$$M(H) = M_s \left(\frac{emu}{g}\right) \int_0^{\infty} L\left(\frac{M(emu/cm^3) V H(Oe)}{k_B T}\right) f(D) dD \quad (4)$$

From a practical point of view, the upper limit for numerical integration of equation (4) corresponds to a high enough diameter (usually 50 nm). Inside the brackets of the Langevin function, physical variables are in gaussian unit. Note that units of $M_s (emu/g)$, should be the same as the experimental one (taken as emu/g in this case). $M_s (emu/g)$ is considered as a variable independent of $M(emu/cm^3)$ (different units are used for clarity). Both variables should be linked by the inorganic content of the sample. In a normal fitting $M(emu/cm^3)$ is fixed a priori, for instance, to the theoretical value of magnetite. In this way, the fit provides a value for the mean size and dispersity, which does not depend on the proper normalization of the experimental magnetization.

Figure S6_a. Fit of $M(H)$ curves at room temperature by SPM model of powder samples (C and E).

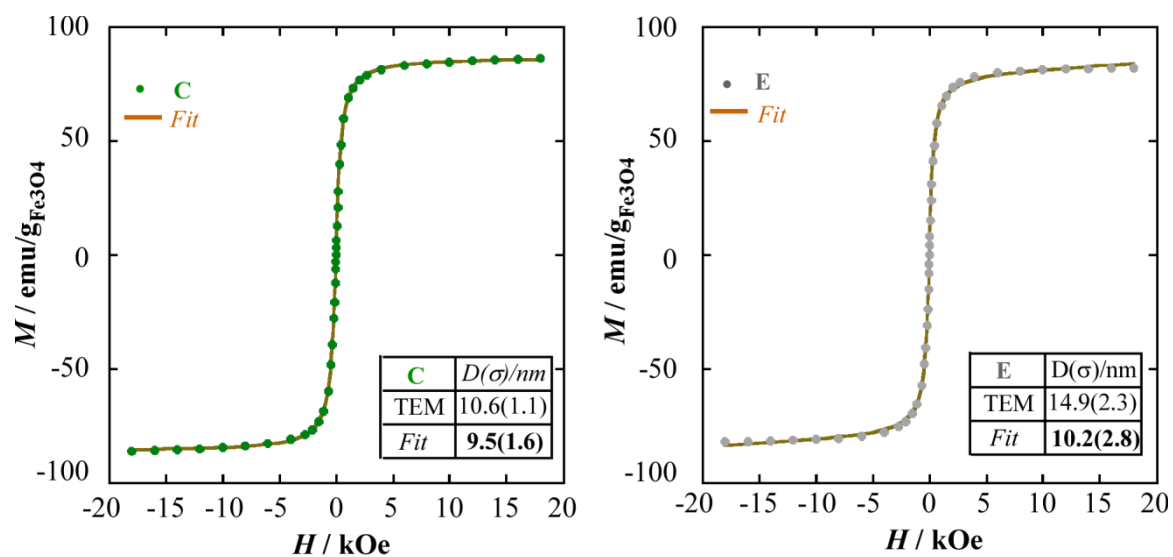
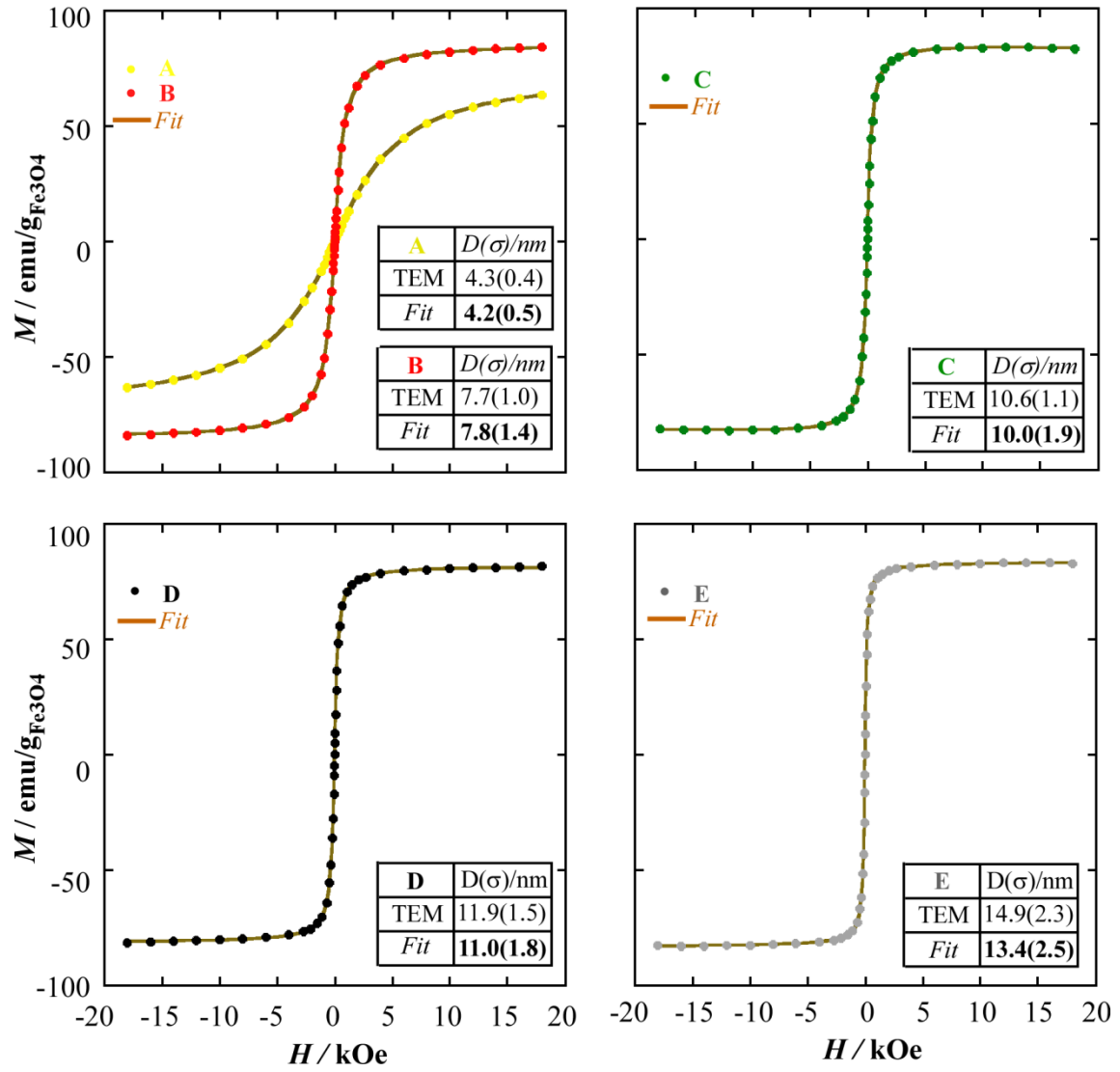


Figure S6_b. Fit of $M(H)$ curves at room temperature by SPM model of colloidal dispersion embedded in polystyrene (A-E).



Model S2. Calculation of SAR as a function of mean diameter.

The value of SAR for any \bar{D} (mean diameter) is calculated by the convolution of SAR versus diameter function, $P_{SPM}(D)$, with a distribution function accounting for size dispersity, $f(D)$:

$$SAR(\bar{D}) = \int_0^{D_{max}} P_{SPM}(D)f(D)dD \quad (5)$$

SAR or absorption power P_{SPM} is given by:

$$P_{SPM} = \mu_0 \pi f \chi'' H^2 \quad (6)$$

where χ'' is the imaginary part of complex susceptibility, and χ_0 the DC susceptibility at low fields:

$$\chi''(\omega) = \chi_0 \frac{\omega \tau_{eff}}{1 + (\omega \tau_{eff})^2} \quad \chi_0 = \frac{\mu_0 M_S^2 V}{3 k_B T} \quad (7)$$

being τ_{eff} , the effective relaxation time, resulting from the superposition of Neel relaxation (τ_N) and Brownian relaxation (τ_B).

$$\frac{1}{\tau_{eff}} = \frac{1}{\tau_N} + \frac{1}{\tau_B} \quad (8)$$

Neel relaxation time can be calculated by:

$$\tau_N = \frac{\tau_0 (\pi k_B T)}{2KV} e^{KV/k_B T} \quad (9)$$

where τ_0 is the inverse of the so-called frequency of jump attempts, usually between 10^{-9} and 10^{-11} s. V is the particle volume, K the effective anisotropy constant and k_B is the Boltzmann constant.

The Brownian relaxation time is given by:

$$\tau_B = \frac{4\pi\eta r_h^3}{k_B T} \quad (10)$$

Where η is the viscosity of the solvent, and r_h the hydrodynamic radius. In the calculation, it is assumed that the effective anisotropy constant is composed of two contributions, $K_v(J/m^3)$, coming from the particle core and $K_s(J/m^2)$ from the shell (or surface):

$$K = K_v + \frac{6K_s}{D} \quad (11)$$

In equation (5) $f(D)$ is any arbitrary distribution of sizes, given in this case by the well known Gaussian function:

$$f(D, \bar{D}, \sigma) = \frac{1}{\sigma\sqrt{2\pi}} \cdot \exp\left(-\frac{(D - \bar{D})^2}{2\sigma^2}\right) \quad (12)$$

where \bar{D} , the mean diameter, and σ , the standard deviation,

Calculation of SAR as a function of mean diameter has been carried out assuming the following parameters

$$T=300 \text{ K}$$

$$H=10 \text{ kA/m}$$

$$f=850 \text{ kHz}$$

$$M_s=450 \text{ kA/m (experimental value at RT, deduced from saturation magnetization)}$$

$$\rho_{\text{Fe}_3\text{O}_4}=5,24 \text{ g/cm}^3$$

$$\eta_{\text{toluene}}=0.55 \text{ mPa}\cdot\text{s}$$

$$D_{\text{hidrod.}} = D_{\text{inorg.}} + l$$

$$K_v=10 \text{ kJ/m}^3$$

$$K_s=15 \text{ }\mu\text{J/m}^2$$

$$\beta=0.15 \text{ (experimental value)}$$

$$\tau_0=10^{-10} \text{ s}$$

Figure S7. SAR values as a function of frequency under an AC magnetic field of 10 kA/m for sample E before and after washing process.

